Effect of Viscosity of an Oil Environment on Fatigue Crack Growth Rate in AISI 316 Stainless Steel

K. BAE and H. CONRAD
Materials Science and Engineering Department, North Carolina State University, Raleigh, NC 27695–7907, USA

ABSTRACT

The effect of viscosity in the range of 10–101500 cS on fatigue crack growth rate, FCGR, ($\Delta K = 11 - 25$ MPa $\sqrt{m}$) in 316 stainless steel tested in silicone oil was investigated and compared with behavior in air. The four orders of magnitude variation in viscosity had no effect on FCGR, nor on the crack opening load P_{op}. The FCGR and P_{op} were smaller in the oils than in air for $\Delta K < \sim 18$ MPa $\sqrt{m}$, but no difference occurred at larger ΔK values. Microscopy observations revealed more zig-zags in the crack path for the air environment compared to the oils; also, cleavage facets on the fracture surface and debris along the crack path occurred in air but not in the oils. It is concluded that the observed difference between FCGR in the oils compared to air results mainly from shielding by the oil of the crack tip against chemical reactions.

KEYWORDS

Fatigue; crack growth; closure; environment; viscosity; zig-zags; cleavage facets; debris.

1. INTRODUCTION

It is well known that the fatigue behavior of metals may be influenced by an oil environment. Studies (Endo et al., 1972, Endo et al., 1972, Frost, 1964, Polk et al., 1975, Ryder et al., 1977, Tzou et al., 1983) on several alloys have shown that Stage II fatigue crack growth rate [FCGR] is lower in oil than in room air. However, when 1 ppm H_2S was added to crude oil, the FCGR in pipeline steels was higher at stress intensity fractor ΔK above 20 MPa $\sqrt{m}$ and lower at ΔK below 20 MPa $\sqrt{m}$, compared to those in air (Vosikovsky, 1976, Vosikovsky et al., 1982). Hydrogen interaction with freshly exposed crack tip was suggested to be responsible for the accelerated FCGR at high ΔK. A corrosion reaction does not however always accelerate the FCGR. A reduced FCGR in a coal slurry-H_2 environment compared to H_2 alone was reported for tests on 2 1/4 Cr–1 Mo steel (Woods et al., 1980). This was attributed to the shielding of the crack tip by the corrosion product from the full effects of the H_2 gas and to their wedging effect on crack closure. In a similar study on 2 1/4 Cr–1 Mo steel and 347 stainless steel (McCabe et al., 1980), sulfide corrosion products wedged the crack open and prevented crack propagation.

In addition to influencing FCGR by shielding the crack tip from air, oils may exert a hydrodynamic wedging action (Endo et al., 1972, Endo et al., 1972, Tzou et al., 1985, Tzou et al., 1985, Way et al., 1935), the degree of which depends on the viscosity. Fluid penetration into the crack forms a wedge and thereby modifies the effective stress amplitude experienced by the crack tip, and consequently the FCGR. Tzou et al. (1985) recently proposed a comprehensive mathematical model for viscosity-induced crack closure, which treated the kinetics of the fluid penetration into the crack and the hydrodynamics of the oil pressure distribution within crack. To interpret the complex fatigue crack growth behavior of 2 1/4 Cr–1 Mo steel in the viscous oils (Tzou et al., 1985), this model was successfully incorporated into the three mutually competitive mechanisms by which viscous oil environments influence FCGR, namely suppression of corrosive reaction, minimization of corrosion-product-induced crack closure and the hydrodynamic wedging action.

Of interest in the present study is the effect of oil viscosity on the FCGR in AISI 316 stainless steel, since this alloy along with 2 1/4 Cr–1 Mo steel is frequently used as a structural component in oil refinery and coal conversion systems.

2. EXPERIMENTAL

The type 316 stainless steel plate (25.4 mm thickness) employed in this study had the composition given in Table 1. As-received plate, which was solution-treated, had a mean

Table 1. Chemical composition of 316 stainless steel plate (25.4 mm thick) in wt.%

Cr 17.15	Mo 2.34	S 0.018	C 0.059
Ni 13.40	Si 0.58	Cu 0.10	N 0.032
Mn 1.84	P 0.024	Co 0.02	

linear intercept grain size of 90 μm and the tensile properties listed in Table 2. CT specimens, conforming to ASTM E–399 with width 35.6 mm and thickness 3.4 mm were machined from the as-received plate to give a TL crack growth orientation. Fatigue crack growth tests were conducted at a constant load amplitude with half sine-wave form (R = 0.05) at a frequency of 4

Table 2. Grain size and mechanical properties in monotonic loading of 316 stainless steel (1).

Grain Size (mm)	Y.S. (0.2%) (MPa)	T.S. (MPa)	El.(2) (%)	R.A. (%)
92	245	542	82 (19 mm)	69

Young's Modulus(3) (GPa)	Hardness(4) VHN (Kg/mm^2)
193	216

Notes:
(1) As-received material.
(2) Number in parentheses is gage length.
(3) Value of Youngs Modulus was obtained from ASM Metals Handbook, 8th Edition, Vol. 1 (1961) p. 423.
(4) Vickers microhardness (100 g load)

Hz in a LFE–150 fatigue machine with its main loading frame in the horizontal position to permit immersion of the specimen in oil environments. A precrack was obtained by the load shedding technique (ASTM E–647, Amzallag et al., 1981), until the final crack length reached about 2.5 mm. All other test conditions conformed to ASTM E–647.

Crack growth tests were performed in: (a) room air (usually 40% to 60% relative humidity) as a reference and (b) silicone oil of 10, 350 and 101500 cS viscosity. Silicone oil was employed because it was considered to be relatively inert. Crack closure was determined from a plot of load (P) versus crack mouth opening displacement (CMOD), which was measured using a clip gage (MTS model 632.01) attached to the specimen mouth. Following the method of Carter et al., 1984), the crack opening load P_{op} was taken when a change in compliance occurred. Crack paths and fracture surfaces were observed by optical and scanning electron microscopy (SEM).

3. RESULTS

Plots of da/dN versus ΔK for silicone oil environments of 10, 350 and 101500 cS along with that for room air are presented in Fig. 1. Evident is that the viscosity of the silicone oil in the

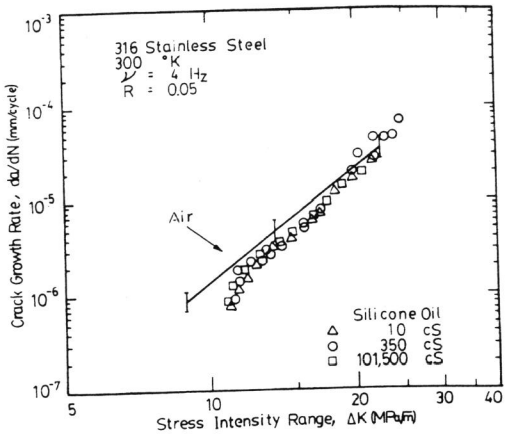

Fig. 1. Effect of the viscosity of silicone oil on fatigue crack growth rate in 316 stainless steel.

range of 10 to 101500 cS does not have a clearly defined effect on the FCGR for the ΔK range considered. However, FCGR in the silicone oils is noticeably lower than in air at ΔK < ~ 18 MPa √m, whereas at higher ΔK the FCGR in the oils is within the scatter of that in air.

Typical load versus CMOD hysteresis loops and the procedure employed to obtain the crack opening load P_{op} are shown in Fig. 2. The variation of P_{op}/P_{max} with ΔK as a function of oil viscosity is presented along with that for room air in Fig. 3. The viscosity of the silicone oil does not have a clear effect on the P_{op}/P_{max} ratio. On the other hand, the P_{op}/P_{max} ratio is higher for air than the viscous oil environments at ΔK < 18 MPa √m. Worthy of mention is that a higher opening load P_{op} at a given ΔK generally yields a lower FCGR, which is opposite to what was observed here (see. Fig. 1).

The nature of the crack path for 316 stainless steel tested in ambient air and silicone oil (350 cS) is shown in Figs. 4 and 5, respectively. Small scale zig-zags, in association with coarse

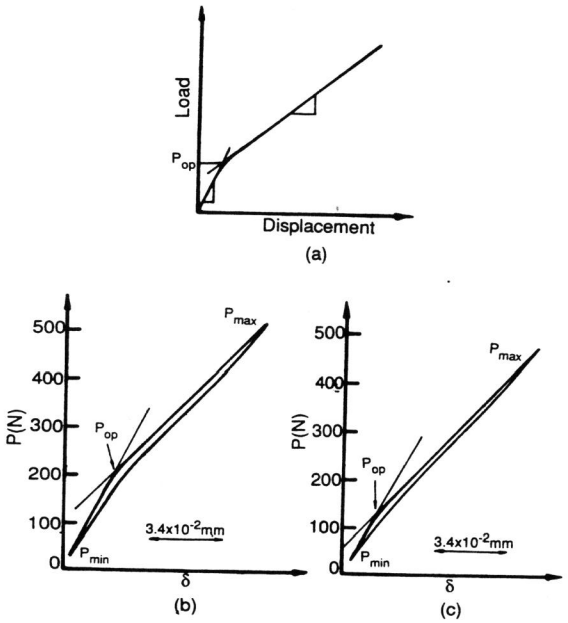

Fig. 2. Measurements of crack closure: (a) schematic of the method for determinng the crack opening load, P_{op}, (b) actual load versus displacement diagram in air at $\Delta K = 11.4$ MPa $\sqrt{m}$ and (c) actual load versus displacement diagram in silicone oil (350 cS) at $\Delta K = 11.3$ MPa $\sqrt{m}$.

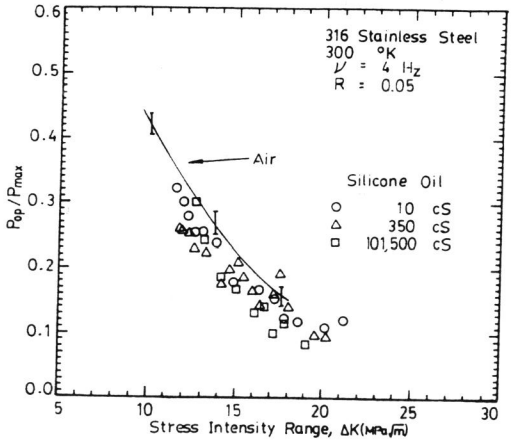

Fig. 3. P_{op}/P_{max} versus ΔK for 316 stainless steel as a function of the viscosity of silicone oil.

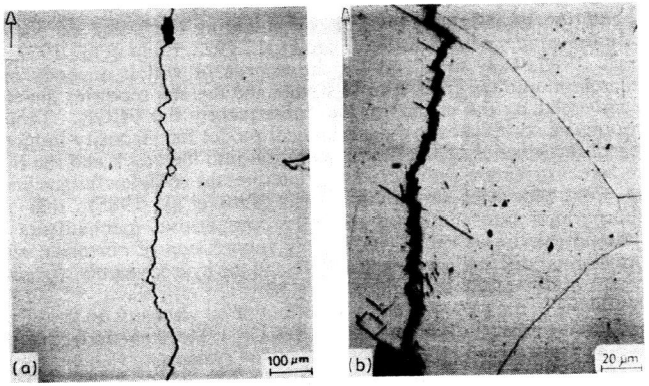

Fig. 4. Nature of fatigue crack path in 316 stainless steel in air at ΔK of (a) 12.3 MPa $\sqrt{m}$ and (b) 12.7 MPa $\sqrt{m}$ (after etching). Arrow indicates crack growth direction and ΔK was calculated at the middle of the micrograph.

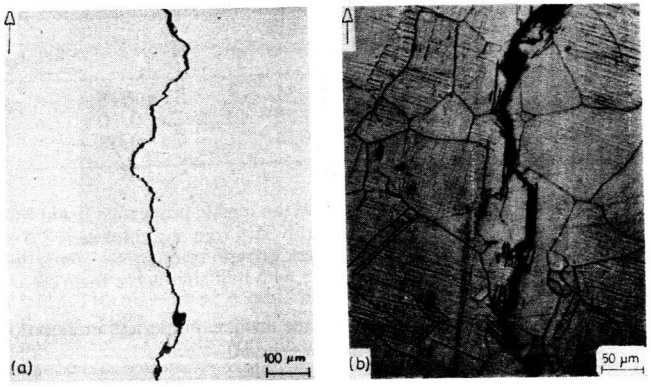

Fig.5. Nature of fatigue crack path in 316 stainless steel in silicone oil (350 cS) at ΔK of (a) 12.2 MPa $\sqrt{m}$ and (b) 12.0 MPa $\sqrt{m}$ (after etching).

slip bands, occur more frequently in the specimen tested in air. Fig. 6 shows the nature of debris observed along the crack on the specimen cycled in air. The debris was readily wiped away with a soft paper tissue as shown in Fig. 6-c. The amount of debris along the crack became less as ΔK increased. The debris was not present on specimens cycled in the silicone oils.

Typical appearance of the fracture surfaces of specimens fatigued in the silicone oils is shown in Fig. 7, revealing a fan-like pattern and a step-pattern roughly along the crack propagation direction. The fracture surfaces of specimens cycled in air (Fig. 8) contained a significant amount of isolated cleavage facets as well as the fan- and step-patterened surface shown in Fig. 7. The mean size of the facets was the order of the grain size. River-patterened parallel bands,

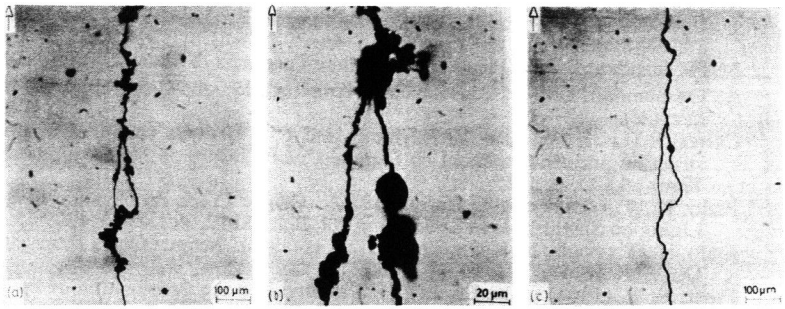

Fig. 6. Debris along fatigue crack in 316 stainless steel cycled in air at ΔK = 10 MPa $\sqrt{m}$ (a) immediately following cycling, (b) at higher magnification and (c) after wiping with tissue paper.

Fig. 7. SEM micrograph of the fracture surface of a specimen tested in silicone oil (350 cS) with ΔK = 12 MPa $\sqrt{m}$.

presumably resulting from the second-order slip, are clearly seen on the facets. Also to be noted in Figs. 7 and 8d are flattened areas associated with physical contact (considered to give surface-roughness-induced closure).

4. DISCUSSION

A four-orders of magnitude variation in the viscosity of the silicone oil had no detectable effect on the FCGR in type 316 stainless steel. This behavior differs from that reported by Tzou et al. (1985) for tests on bainitic 2 1/4 Cr–1 Mo steel. They found that FCGR in inert oils increased in the order of their viscosity and attributed this to viscosity-induced hydrodynamic wedging action on crack closure. The present crack closure results indicate an essentially constant level of crack closure in the silicone oils, which ranged in viscosity from 10 to 101, 500 cS. Worthy of mention in this regard is that the hydrodynamic wedging mechanism is generally regarded less potent compared to other closure sources, such as corrosion debris and fracture surface roughness, in influencing the FCGR (Tzou et al., 1985).

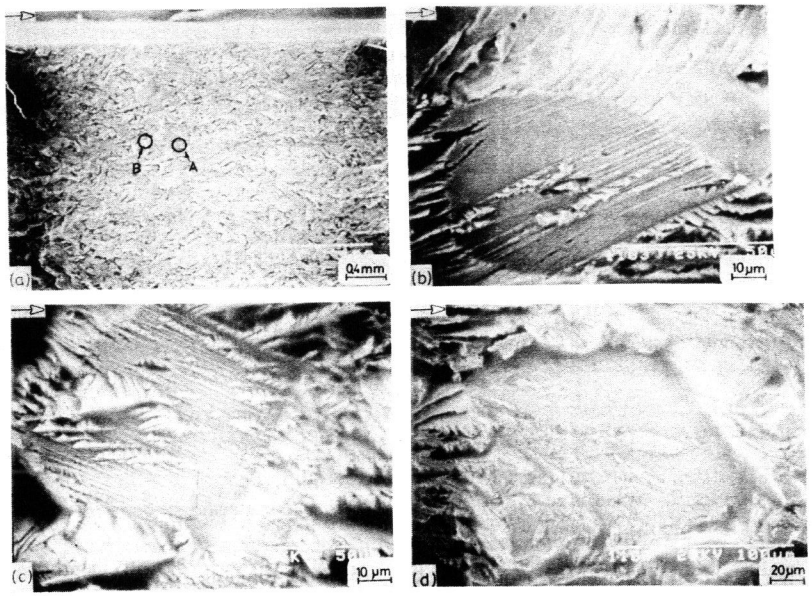

Fig. 8. SEM micrographs of the fracture surface of a specimen tested in air: (a) ΔK = 9.55 MPa $\sqrt{m}$, (b,c) magnified views of A and B respectively in (a) and (d) ΔK = 12 MPa $\sqrt{m}$.

Crack advances in certain microstructures at low ΔK take place primarily along a single active slip system Minakawa et al., 1981, Suresh et al., 1984). Such single-shear growth, which occurs primarily when the maximum plastic zone size is typically smaller than the grain size, results in: (a) crystallographic or generally faceted fracture features, (b) an irregular surface morphology and (c) locally mixed Mode I and II crack growth (Carter et al., 1984, Minakawa et al., 1981, Suresh, 1983, Suresh et al., 1984). This often leads to a mismatch between the fracture surface asperities during the unloading portion of the fatigue cycle, resulting in a roughness-induced crack closure. This type of closure is pronounced in coarse-grained, planar slip material, and enhanced by oxidation of slip steps (Gray III et al., 1983). The present fatigue crack growth behavior in 316 stainless steel is in accord with these conditions. The high crack closure level observed in the low ΔK region in both silicone oil and air thus appears to be mainly due to fracture surface roughness. Flattened regions in SEM micrographs in Fig. 7 and 8-c support this view.

Corrosion products formed within growing cracks can also cause crack closure. Moist atmosphere often forms an oxide film within the crack, which further thickens by fretting oxidation (Gray III et al., 1983, Tzou et al., 1985). This mechanism is usually specific to the low ΔK range, where the oxide thickness is of the order of the crack tip opening displacement. Therefore, the debris along the crack observed only in the air at the low ΔK in the present study may be the result of fretting oxidation. Slightly higher P_{op}/P_{max} in air compared to that in silicone oils is thus probably due to the oxide-induced closure. Conditions which may be present at the crack tip for air and oil environments are schematically compared in Fig. 9.

Since the closure load levels were lower in the silicone oils, the effective stress intensity range ΔK_{eff} must be higher, which would give a higher FCGR in oils. But in the present tests at low

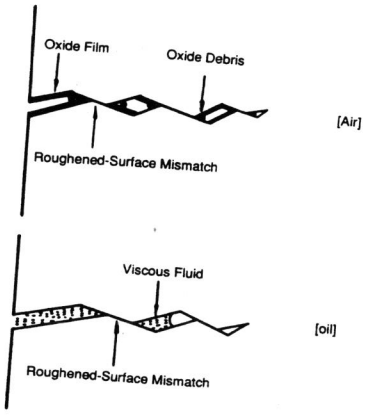

Fig. 9. Schematic of conditions at crack tip for air and silicone oil environments.

ΔK, the FCGR was in fact lower in silicone oils. This means that the mechanical influence of crack closure on the FCGR (Gray III et al., 1983) was overshadowed by the shielding effect of the oil at the crack tip. Evidence for the suppression of chemical activity at the crack tip in silicone oils is provided by the absence of the debris and cleavage facets which were observed for tests in air.

5. SUMMARY AND CONCLUSIONS

1. A four-orders of magnitude variation in the viscosity of silicone oil had no detectable effect on the crack closure level and the FCGR in type 316 stainless steel.
2. FCGR in silicone oil was lower than in air at $\Delta K < \sim 18$ MPa $\sqrt{m}$, but was the same as that in air at higher ΔK.
3. High closure loads observed at low ΔK in both oils and air appear to be due to the fracture surface roughness.
4. The slightly lower closure loads in the oils compared to air had no significant effect on the FCGR.
5. Shielding from moist air-induced chemical reactions at the crack tip is proposed to be a major factor for the lower FCGR in silicone oils.
6. The combined opposite effects of a lower closure load and shielding from the air environment by the oils yielded a lower FCGR in the oils compared to air at $\Delta K < 18$ MPa $\sqrt{m}$.

ACKNOWLEDGEMENT

This research was sponsored by the Department of Energy under Contract DE-FG22-80PC30236.

REFERENCES

Amzallag, C., P. Rabbe, C. Bathias, D. Benoitt and M. Truchon (1981). Influence of Various Parameters on the Determination of the Fatigue Crack Arrest Threshold, ASTM STP 738, p. 29.

ASTM Standard E–399 (Plane-Strain Fracture Toughness of Metallic Materials).

ASTM Standard E–647 (Constant-Load-Amplitude Fatigue Crack Growth Rate Above 10^{-8} m/cycle).

Carter, R.D., E. W. Lee, E. A. Starke and C. J. Beevers (1984). The Effect of Microstructure and Environment on Fatigue Crack Closure of 7475 Aluminum Alloy, Met. Trans., 15A , p. 555.

Endo, K., T. Okada and T. Hariya (1972). Fatigue Crack Propagation in Bearing Metals Lining on Steel Plates in Lubricating Oil, Bull. JSME, Vol. 15, p. 439.

Endo, K., T. Okada, K. Komai and M. Kiyota (1972). Fatigue Crack Propagation of Steel in Oil, Bull. JSME, Vol. 15, p. 1316.

Frost, N. E. (1964). The Effect of Environment on the Propagation of Fatigue Cracks in Mild Steel, Appl. Matls. Res., 3, p. 131.

Gray III, G. T., A. W. Thompson and J. C. Williams (1983). The Effect of Microstructure on Fatigue Crack Path, In: Fatigue Crack Growth Threshold Concepts, p. 131, The Met Soc. of AIME.

McCabe, D. E. and J. D. Landes (1980). Design Properties of Steels for Coal Conversion Vessels, Final Rep. EPRI AP–1637, Nov. 1980 (Electric Power Research Inst.) (Research Project 627–1).

Minakawa K. and A. J. McEvily (1981), On Crack Closure in the Near-Threshold Region, Scripta Met., 15, p. 633.

Polk, C. J., W. R. Murphy and C. N. Rowe (1975). Determining Fatigue Crack Propagation Rates in Lubricating Environments Through the Application of a Fracture Mechanics Technique, ASLE Trans., 18, p. 290.

Ryder, D. A., M. Martin and M. Abdullah (1977). Some Factors Influencing Stage 1 Fatigue–Crack Growth, Metal. Sci., 11, p. 340.

Suresh S. and R. O. (1984). Ritchie Propagation of Short Fatigue Cracks, International Metals Reviews, 29, p. 445.

Suresh, S.(1983). Crack Deflection: Implications for the Growth of Long and Short Fatigue Cracks, Met. Trans., 14A, p. 2375.

Suresh, S. and R. O. Ritchie (1983). Near-Threshold Fatigue Crack Propagation: A Perspective on the Role of Crack Closure, In: Fatigue Crack Growth Threshold Concepts, p. 227, The Met. Soc. of AIME.

Tzou, J. L., S. Suresh and R. O. Ritchie (1983). Fatigue Crack Propagation in Viscous Environemnts, In: Mech. Behaviour of Materials - IV, (J. Carlsson and N. G. Ohlson, eds.Vol. 2, p. 711 Pergamon Press, NY.

Tzou, J. L., S. Suresh and R. O. Ritchie (1985). Fatigue Crack Propagation in Oil Environments — I. Crack Growth Behavior in Silicone and Paraffin Oils, Acta Met., 33, p. 105.

Tzou, J. L., C. H. Hsueh, A. G. Evans and R. O. Ritchie (1985). Fatigue Crack Propagation in Oil Environments — II. A Model for Crack Closure Induced by Viscous Fluids, Acta Met., 33, p. 117.

Vosikovsky, O. (1976). Fatigue Crack Growth in an X65 Line-Pipe Steel in Sour Crude Oil, Corrosion, 32, p. 472.

Vosikovsky, O. and A. Rivard (1982). The Effect of Hydrogen Sulfide in Crude Oil on Fatigue Crack Growth in a Pipe Line Steel, Corrosion, 38, p. 19.

Way, S., J.(1935). Pitting Due to Rolling Contact, Appl. Mech., Trans. ASME Series E, 2, p. A49.

Wood, C. M., T. E. Scott and O. Buck, Alloy Evaluation for Fossil Fuel Process Plants (Liquefaction), Annual Rep., Oct. 1, 1980 ~ Sept. 30, 1981.